Atomic-scale insights of indium segregation and its suppression by GaAs insertion layer in InGaAs/AlGaAs multiple quantum wells

Shu-Fang Ma(马淑芳)[1,†], Lei Li(李磊)[1,2], Qing-Bo Kong(孔庆波)[1,2], Yang Xu(徐阳)[1,2], Qing-Ming Liu(刘青明)[1,2], Shuai Zhang(张帅)[1,2], Xi-Shu Zhang(张西数)[1,2], Bin Han(韩斌)[1], Bo-Cang Qiu(仇伯仓)[1], Bing-She Xu(许并社)[1,3,‡], and Xiao-Dong Hao(郝晓东)[1,§]

[1] *Materials Institute of Atomic and Molecular Science, Shaanxi University of Science and Technology, Xi'an* 710021, *China*
[2] *School of Materials Science and Engineering, Shaanxi University of Science and Technology, Xi'an* 710021, *China*
[3] *Key Laboratory of Interface Science and Engineering in Advanced Materials, Taiyuan University of Technology, Taiyuan* 030024, *China*

(Received 2 March 2022; revised manuscript received 9 May 2022; accepted manuscript online 18 May 2022)

The In segregation and its suppression in InGaAs/AlGaAs quantum well are investigated by using high-resolution x-ray diffraction (XRD) and photoluminescence (PL), combined with the state-of-the-art aberration corrected scanning transmission electron microscopy (Cs-STEM) techniques. To facility our study, we grow two multiple quantum wells (MQWs) samples, which are almost identical except that in sample B a thin GaAs layer is inserted in each of the InGaAs well and AlGaAs barrier layer comparing to pristine InGaAs/AlGaAs MQWs (sample A). Our study indeed shows the direct evidences that In segregation occurs in the InGaAs/AlGaAs interface, and the effect of the GaAs insertion layer on suppressing the segregation of In atoms is also demonstrated on the atomic-scale. Therefore, the atomic-scale insights are provided to understand the segregation behavior of In atoms and to unravel the underlying mechanism of the effect of GaAs insertion layer on the improvement of crystallinity, interface roughness, and further an enhanced optical performance of InGaAs/AlGaAs QWs.

Keywords: InGaAs/AlGaAs quantum well, GaAs insertion layer, In segregation, scanning transmission electron microscopy

PACS: 78.20.–e, 07.79.–v, 68.37.Ma **DOI:** 10.1088/1674-1056/ac70b5

1. Introduction

InGaAs/AlGaAs strained quantum wells (QWs) are widely used in semiconductor quantum well laser devices for the emission wavelength range from around 830 nm to about 1100 nm.[1–3] Obviously, it is important to grow the QWs with high quality so that a better device performance, such as internal quantum efficiency and reliability, can be obtained. High quality InGaAs/(Al)GaAs QWs with an abrupt elemental distribution of In atoms at the interface of the well–barrier layers, as well as perfect crystal quality, are usually grown by well-developed MBE and MOCVD systems.[4–8] The preferential segregation of In atoms at the well–barrier interface has been found to increase the interface flocculation and to transform the growth mode from the two-dimensional to three-dimensional mode.[9–12] Thus, it is highly desirable to suppress the segregation of In atom in InGaAs/AlGaAs QWs.

To prevent the segregation of In elements at the well–barrier interface of InGaAs/AlGaAs QWs, a number of approaches have been developed. One way was to precisely control on the growth temperature of epitaxial layers owning to the fact that appropriate growth temperature for InGaAs and AlGaAs is different.[13] A relatively higher temperature may be needed to remove the impurity and promote the high migration ability of Al atoms.[14] Whereas, the segregation length of In atom will be increased when the growth temperature exceeds 600 °C in the MOCVD growth process.[6] An alternative approach was to insert a thin layer between the well–barrier interface to prevent the atomic segregation without adjusting the growth temperature. It was reported that a thin GaAs layer was chosen as the ideal candidate to improve the interface roughness and enhance the device performance.[7,15–17] For instance, Wen *et al.* reported the intercalation of GaAs layer into the InGaAs/GaAsP strained QWs with achieved improved abruptness at the interfaces.[15] Very recently, Zhang *et al.* studied the effect of GaAs insertion layer on the optical properties of InGaAs/AlGaAs QWs by optimizing the thickness of GaAs.[18] Whereas, since the atomic-resolution of the interfacial structure is challenging to observe, especially the biasing behavior of In elements at the well–barrier interface, the atomistic effect of GaAs insertion layer on improving the interface structure quality is still limited.

2. Design

Aiming at underlying the mechanism of effect of GaAs insertion layer on improving the interface quality and optical performance, study of the segregation behavior of In at the

[†]Corresponding author. E-mail: mashufang@sust.edu.cn
[‡]Corresponding author. E-mail: xubs@tyut.edu.cn
[§]Corresponding author. E-mail: hao.xiaodong@sust.edu.cn

© 2023 Chinese Physical Society and IOP Publishing Ltd

well–barrier interface is essential. In this regard, the state-of-the-art aberration-corrected scanning transmission electron microscopy (Cs-STEM) is employed to obtain better insights into the interface structure in the atomic scale. In this study, two MQWs samples were grown on ⟨001⟩ oriented n-type GaAs substrates by MOCVD method in an Aixtron 2800 G4-TM (C2) system at the temperature of 650 °C (see details in supplementary materials method). The structures (Fig. 1) show that a thin GaAs layer is inserted in the interface of the InGaAs/AlGaAs MQWs. The direct observation of the inhomogeneous distribution of In atoms within the well and barrier layers in InGaAs/AlGaAs QWs are achieved. In addition, it clearly demonstrated that the segregation of In atoms is mainly suppressed within the thin inserted GaAs layer. Therefore, the GaAs insertion layer is mainly responsible for the improvement of the crystal quality, interface roughness, and optical performance.

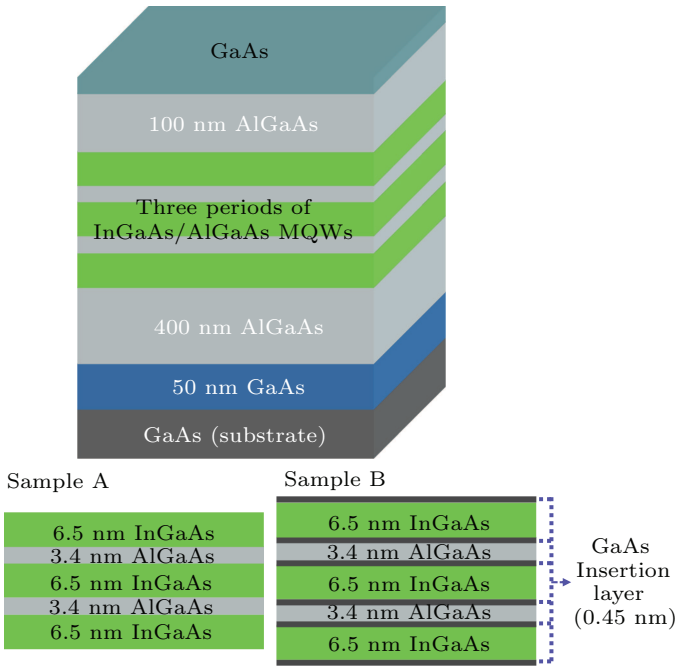


Fig. 1. Schematic illustration of the epitaxial layers of InGaAs/AlGaAs MQWs (sample A) and InGaAs/GaAs/AlGaAs MQWs (sample B).

3. Results and discussion

As can be seen in Fig. 2(a), in the symmetric (004) HRXRD ω–2θ scan curve of sample B (InGaAs/GaAs/AlGaAs MQWs), the presence of tertiary satellite peaks is clearly observed, while for sample A (InGaAs/AlGaAs MQWs) only the secondary satellite peaks can be seen at most. In addition, the satellite peak of sample B displays higher peak intensities, narrower full widths at half maximum (FWHM) than that of the sample A. By comparing the satellite peaks of the two structures, the curve of sample B shows the fringe peaks with obvious boundaries and high intensities, indicating that the presence of GaAs intercalation layer significantly improves the crystal quality of InGaAs/AlGaAs MQWs.[19–21] Meanwhile, the thickness and concentration of In (Al) elements in the epitaxial layers in these two samples are analyzed, and the data was shown in Table S1. It is found that the In content in the InGaAs well layers of sample B is higher than that of the sample A. In contrast, the segregation of In atoms in sample A seems severe, which leads to a lower In content in each InGaAs layers. It also shows that the thickness of the epitaxial layers in sample B is more uniform after the insertion of GaAs layer compared to that of sample A, and for epitaxial wafers, the uniform thickness represents a better crystal quality, which is beneficial to obtain a more stable luminescence. The thickness of GaAs insertion layer is simulated to be approximately 0.45 nm. Moreover, the distance between the 0th-peak and the substrate peak of both samples were also derived as 3.8379 arcsec and 2.4623 arcsec. Considering that the lattice strain increases along with the introduction of In content, this distance should become larger in sample B owing to a larger In content in the well layer. However, the presence of GaAs insertion layer seems to smooth the interface and compensates the lattice strain in some extent, leading to the a closer distance between the 0th-peaks peak and the substrate peak in sample B.

To examine the interface quality of these two samples, the FWHM plot as a function of peak order is also shown in Fig. 2(b). The FWHM of the nth satellite peak can be expressed by the following formula:[22]

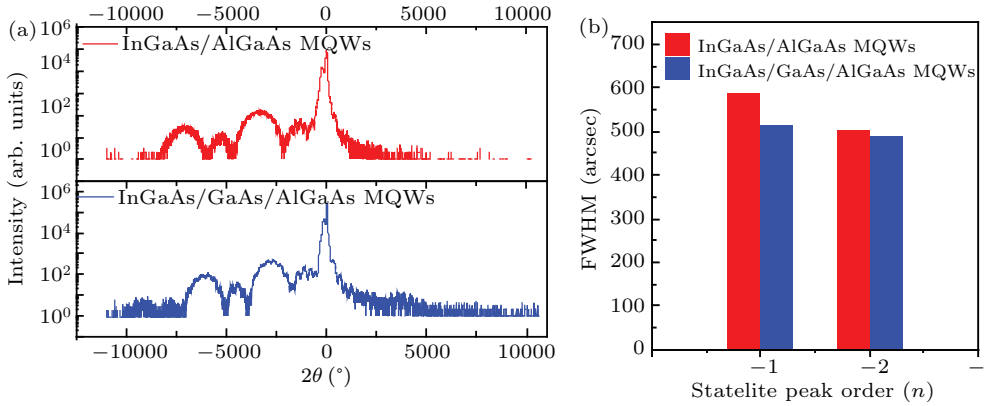


Fig. 2. (a) and (b) The ω–2θ scans measured around the (004) symmetric HRXRD patterns.

$$\omega_n = \omega_0 + (\ln 2)^{1/2} \cdot n\Delta\theta_m \cdot \theta/\Lambda_0, \quad (1)$$

where n is the order of the satellite peak, ω_n is the FWHM of the nth order satellite peak, ω_0 is the zeroth order satellite peak, $\Delta\theta_m$ is the angle spacing between the adjacent satellite peaks, and σ/Λ_0 is the interface roughness of QWs and barriers. The dependence of the FWHM of satellite peaks on the satellite orders shows a linear relationship. It is obvious that the slope of fitting curve of sample B is lower than that of sample A, which demonstrates that the interface fluctuation and roughness of sample B is reduced. The compressive strain brought by In surface segregation might be one of the reasons to a shift toward a lower diffraction angle of satellite peaks.[23] The result indicates that the GaAs insertion layer significantly decreases the In segregation to form a smooth and uniform interface, and ensures the crystal quality of MQWs.[24]

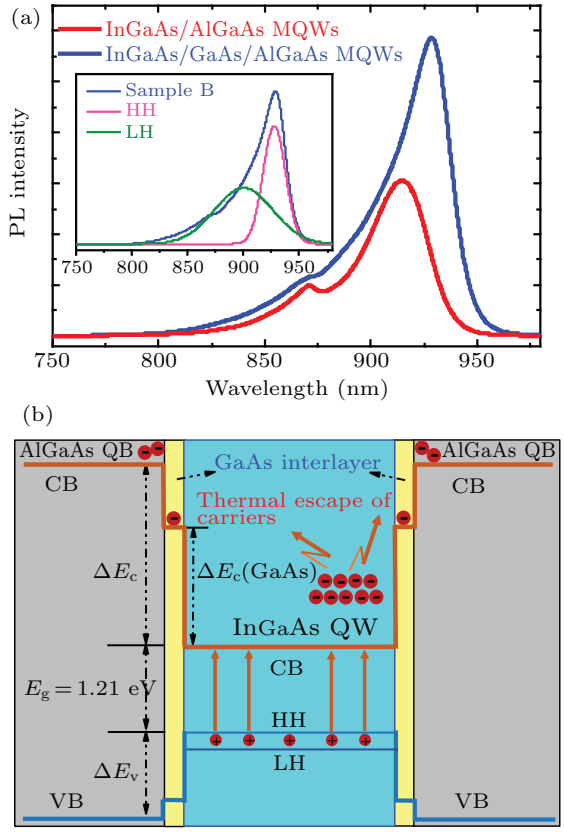


Fig. 3. (a) Photoluminescence spectra of InGaAs/AlGaAs MQWs and InGaAs/GaAs/AlGaAs MQWs at 300 K. The inset shows the multi-peaks Gaussian fitting of the PL spectra of InGaAs/GaAs/AlGaAs MQW. (b) The corresponding band diagram of InGaAs/GaAs/AlGaAs QW.

Figure 3(a) shows the photoluminescence (PL) spectra of the two MQWs samples with identical pumping laser power at 532 nm measured at 300 K. For the sample A, the emission peak locates at around 915 nm, accompanied with a small peak at around 871 nm which can be indexed to the peak of GaAs substrate.[25] As expected, the emission peak red shifts to 927 nm after the insertion of GaAs insertion layer in sample B. It is well known that the band gap of InGaAs is related to the In composition in the well layer. Based on the above XRD analysis, it is clear In content in the QW layer of sample B is relatively larger than that in sample A. Thus, the larger In fraction in InGaAs QW leads to a smaller band gap in sample B, corresponding to the red-shift of PL peak position. Moreover, the FWHM of PL spectra is reduced from 24.1 nm to 20.0 nm, which is in consist with the improved crystal quality and interface roughness by the suppression of In ingredients within the well layers.[26–28] In addition, the asymmetry of PL peak as discussed in Fig. S2 is due to the radiation recombination of the ground state electron-light hole band in InGaAs strained MQWs.[18] Whereas, the thermal escape of carriers is likely to take place from the InGaAs QWs due to the lower GaAs potential barrier than that of AlGaAs, which could reduce the probability of radiation recombination in QWs and lead to the decreased PL intensity, as illustrated in the energy band diagram in Fig. 3(b).[29] It is supposed that the suppression of In segregation by the GaAs insertion layer plays a more significant role in the effect of the optical properties of the InGaAs/AlGaAs MQWs structure. Thus, the non-radiative recombination is largely suppressed and the integral strength of PL for InGaAs/GaAs/AlGaAs MQWs is still increased compared with InGaAs/AlGaAs MQWs as a result.[18,30]

After understanding the improved optical performance by the GaAs insertion layer in the InGaAs/AlGaAs MQWs, one would curious to know how can such a thin layer of GaAs prevent the segregation of In atoms at the well–barrier interface. For this purpose, the state-of-the-art Cs-STEM techniques were utilized. At the beginning, the cross-sectional low magnification STEM images, combined with the STEM-EDS elemental mapping were recorded to examine the distribution of In atoms within the QWs, as shown in Fig. S2. It is clear In atoms distribute not uniform within the well layer and they diffuse to the barrier layers in a large amount in many regions in sample A. However, for sample B, the In atoms locate mainly within the well layers and distribute relatively homogenous comparing to that of sample A. These results are in consistent with the data derived from XRD that the calculated In content in three well layers are relatively higher in sample B than that of in sample A. Moreover, to obtain a deeper insight into the influence of the interfacial structure on crystal quality and optical properties, as well as to visualize the relationship between interfacial structure and In segregation behavior, atomic-scale and more detailed characterization of these two samples were performed. It is well known that in the STEM image mode, the ABF image is able to resolve the light and heavy elements simultaneously, compared to the Z-sensitive HAADF image that only heavy atoms are clearly resolved.[31–36] Comparatively, as shown in Fig. 4 that the interface structure is much improved via the intercalation of the thin GaAs layer. In detail, it shows a brighter intensity in the regions marked by the dotted

line in the colored HAADF image Fig. 4(b), indicating that In segregation occurs not only in the well layers, but is extended into the barrier layers. Such kind of segregation is frequently seen as showed in the low magnification image in ABF-STEM image in Fig. 4(a), where the "dumbbell" shape of Ga(In)/As columns becomes blurred in the dark regions marked by the red dotted circle.

Moreover, the intensity profiles are recorded for a clear demonstration of In distribution along one representative atomic layer as showed in the red and blue box in Figs. 4(b) and 4(d), respectively. The different layers can be easily indexed considering the Z-sensitive dumbbell intensity of Ga(In)/As, Ga/As, and Ga(Al)/As marked by the colored boxes filled in the intensity profiles. For sample A in Fig. 4(e), the dumbbell of Ga(In, Al)/As columns are fluctuated that many minor peaks exist around the main peaks. These results demonstrate that the nonuniform distribution of In atoms occurs within the InGaAs well layer, and In atoms diffuse from its initial atomic position thus the profile becomes broader for some atomic layers pointed by white arrow in the dotted rectangle region. After the intercalation of GaAs insertion layer, the intensity profiles become relatively sharper and smoother in the sample B in Fig. 4(f). In addition, it shows an abrupt transition at the InGaAs/GaAs interface from a higher intensity of Ga(In) column (pointed by white arrow) than As column to an almost even intensity, suggesting that the In segregation is mainly suppressed by the intercalation of GaAs insertion layer. But there is still a minority of In atoms diffuse into the GaAs insertion layer that the intensity profile of first insertion layer (GaAs-I) is slightly broader than the third layer (GaAs-III). Therefore, the calculated thickness of the GaAs insertion layer (approximately 0.57 nm) is slightly broader than the initially design owing to the small amount of In diffusion. After that, the structure–property relationship becomes clear in the atomic scale, indicating that the GaAs insertion layer plays a dominant role in suppressing the segregation of In atoms as showed in the above STEM characterization results, and subsequently inhibiting the formation of InAlGaAs quaternary alloy at the well–barrier interface.

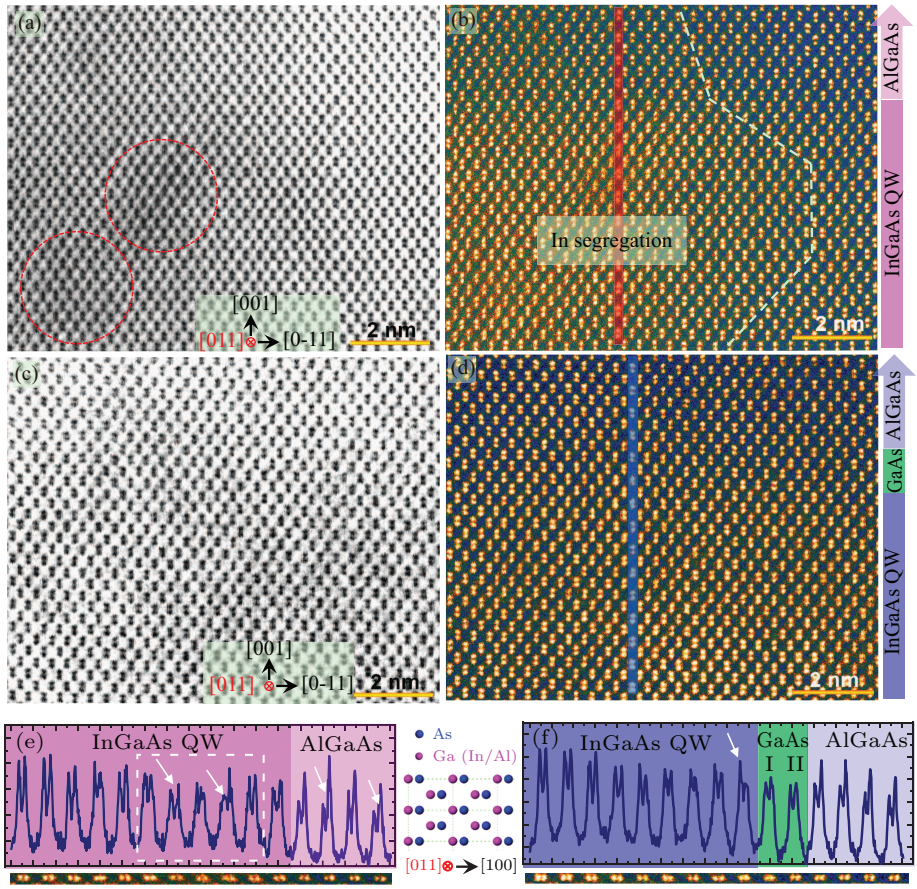


Fig. 4. Atomic-scale ABF- and HAADF-STEM images of (a), (b) InGaAs/AlGaAs MQWs and (c), (d) InGaAs/GaAs/AlGaAs MQWs along [011] projection; (e), (f) the corresponding line intensity profiles along the red and blue boxes in (b), (d) respectively. The arrow in the right side indicates the grow direction of [100].

4. Conclusion and perspectives

In summary, it is essential to reveal the segregation behavior of In atoms in InGaAs/AlGaAs QWs and subsequently improve the interface structure and optical performance by the suppressing the segregation of In atoms within QWs. In this regard, a thin GaAs layer has been inserted to InGaAs/AlGaAs QWs by the MOCVD method. The HRXRD data, com-

bined with the EDS mapping and the atomic-scale resolved ABF- and HAADF-STEM images, have provided the direct and substantial evidences for the segregation behavior of In atoms at the InGaAs/AlGaAs QWs interface, and the effect of the GaAs insertion layer on the suppression of In segregation in the atomic scale. As expected, the improved interface roughness and crystal quality are achieved after the insertion of GaAs layer in InGaAs/AlGaAs QWs, leading to the enhanced optical performance. Such kind of atomic-scale investigations on the interface structure of MQWs could, in principle, be generalized to uncover the underlying mechanism of structure-property issues in the III–V group semiconductor epitaxy films.

Acknowledgements

X. H. gratefully acknowledges the financial support from the National Natural Science Foundation of China (Grant No. 21902096) and the Scientific Research Foundation of Shaanxi University of Science and Technology (Grant No. 126061803). S. M. and B. X. thank the National Natural Science Foundation of China (Grant No. 21972103) and the Shanxi Provincial Key Innovative Research Team in Science and Technology (Grant No. 201703D111026).

References

[1] Moser A, Oosenbrug A, Latta E, Forster T and Gasser M 1991 *Appl. Phys. Lett.* **59** 2642
[2] Sin Y, Lingley Z, Presser N, Brodie M, Ives N and Moss S C 2017 *IEEE. J. Sel. Top. Quant.* **23** 1500813
[3] Zhang P, Song Y, Tian J, Zhang X and Zhang Z 2009 *J. Appl. Phys.* **105** 053103
[4] Gerard J M and Le Roux G 1993 *Appl. Phys. Lett.* **62** 3452
[5] Kaspi R and Evans K R 1995 *Appl. Phys. Lett.* **67** 819
[6] Marmalyuk A, Govorkov O, Petrovsky A, Nikitin D, Padalitsa A, Bulaev P, Budkin I and Zalevsky I 2002 *J. Cryst. Growth.* **237** 264
[7] Yuan H, Li L, Zhang J, Li Z, Zeng L, Wang Y, Qu Y, Ma X and Liu G 2019 *Optik* **176** 295
[8] Chen S, Li W, Wu J, Jiang Q, Tang M, Shutts S, Elliott S N, Sobiesierski A, Seeds A J, Ross I, Smowton P M and Liu H 2016 *Nat. Photonics* **10** 307
[9] Froyen S and Zunger A 1996 *Phys. Rev. B* **53** 4570
[10] Toyoshima H, Niwa T, Yamazaki J and Okamoto A 1993 *Appl. Phys. Lett.* **63** 821
[11] Ohtake A, Ozeki M, Terauchi M, Sato F and Tanaka M 2002 *Appl. Phys. Lett.* **80** 3931
[12] Schowalter M, Rosenauer A and Gerthsen D 2006 *Appl. Phys. Lett.* **88** 111906
[13] Huo D Y, Shi Z W, Zhang W, Tang S L and Peng C S 2017 *Acta Phys. Sin.* **66** 068510 (in Chinese)
[14] He Z, Wang H, Wang Q, Fan J, Zou Y and Ma X 2020 *Opt. Mater* **108** 110227
[15] Wen Y, Wang Y and Nakano Y 2012 *Appl. Phys. Lett.* **100** 053902
[16] Wen Y, Wang Y, Watanabe K, Sugiyama M and Nakano Y 2011 *Appl. Phys. Express* **4** 122301
[17] Xu K, Huang L, Zhang Z, Zhao J, Zhang Z, Snyman L W and Swart J W 2018 *Mat. Sci. Eng. B-Adv.* **231** 28
[18] Zhang B, Wang H, Wang X, Wang Q, Fan J, Zou Y and Ma X 2021 *J. Alloy. Compd.* **872** 159470
[19] He X and Razeghi M 1993 *J. Appl. Phys.* **73** 3284
[20] Dong H, Sun J, Ma S, Liang J, Lu T, Liu X and Xu B 2016 *Nanoscale* **8** 6043
[21] Huynh S H, Ha M T H, Do H B, Nguyen T A, Luc Q H and Chang E Y 2018 *Appl. Phys. Express* **11** 045503
[22] Pan Z, Wang Y, Zhuang Y, Lin Y, Zhou Z, Li L, Wu R and Wang Q 1999 *Appl. Phys. Lett.* **75** 223
[23] Wang C, Goyal A, Menzel S, Calawa D, Spencer M, Connors M, McNulty D, Sanchez A, Turner G and Capasso F 2013 *J. Cryst. Growth.* **370** 212
[24] Fujii H, Wang Y, Watanabe K, Sugiyama M and Nakano Y 2012 *J. Cryst. Growth.* **352** 239
[25] Huang J Y, Shang L, Ma S F, Han B, Wei G D, Liu Q M, Hao X D, Shan H S and Xu B S 2020 *Chin. Phys. B* **29** 010703
[26] Zhao Y, Huang J, Sun Y, Yu S, Li K and Dong J 2019 *Appl. Phys. A-Mater.* **125** 117
[27] Singh J and Bajaj K K 1985 *J. Appl. Phys.* **57** 5433
[28] Chen Y, Xu D, Xu K, Zhang N, Liu S, Zhao J, Luo Q, Snyman L W and Swart J W 2019 *Chin. Phys. B* **28** 107801
[29] Dong H, Sun J, Ma S, Liang J, Lu T, Jia Z, Liu X and Xu B 2016 *Phys. Chem. Chem. Phys.* **18** 6901
[30] Weman H, Sirigu L, Karlsson K F, Leifer K, Rudra A and Kapon E 2002 *Appl. Phys. Lett.* **81** 2839
[31] Findlay S D, Shibata N, Sawada H, Okunishi E, Kondo Y and Ikuhara Y 2010 *Ultramicroscopy* **110** 903
[32] Hao X, Chen C, Saito M, Yin D, Inoue K, Takami S, Adschiri T and Ikuhara Y 2018 *Small* **14** 1801093
[33] Hao X, Zhang S, Xu Y, Tang L, Inoue K, Saito M, Ma S, Chen C, Xu B, Adschiri T and Ikuhara Y 2021 *Nanoscale* **13** 10393
[34] Beyer A and Volz K 2019 *Adv. Mater. Interfaces* **6** 1801951
[35] Han H, Beyer A, Jandieri K, Gries K, Duschek L, Stolz W and Volz K 2015 *Micron* **79** 1
[36] Liu Q, Han D, Ma S, Hao X, Wei Y, Cao B, Zhang S, Hou Y, Shang L, Han B, Shan H, Yang Y and Xu B 2020 *Appl. Phys. Lett.* **117** 212103